(Received 1 January 2026, Accepted 2 February 2026, Scheduled 17 March 2026)

A New Hybrid Approach Based on ANN and z-Transformation for RIS Unit Cells Characterization

Marwah A. Naser[1, 2], Jit S. Mandeep[2], Taha A. Elwi[3, *], and Mohammad T. Islam[2, 4]

[1] *Department of Computer Engineering, College of Engineering, University of Baghdad, Baghdad, Iraq*
[2] *Department of Electrical, Electronic and System Engineering*
Faculty of Engineering & Built Environment (FKaB), Universiti Kebangsaan Malaysia (UKM), Malaysia
[3] *Department of Automation and Artificial Intelligence Engineering*
College of Information Engineering at Al-Nahrain University, Baghdad, Iraq
[3] *Computer and Information Sciences Research Center (CISRC)*
Imam Mohammad Ibn Saud Islamic University (IMSIU), Riyadh, Saudi Arabia

ABSTRACT: Integrating Reconfigurable Intelligent Surfaces (RIS) with wideband systems, such as millimeter-wave (mm-wave) and terahertz (THz) systems, has shown great potential for improving communication system performance. However, accurate circuit-level modeling of the RIS unit cell remains to date a significant challenge. This is because the unit cell in wideband systems faces a strongly coupled electromagnetic behavior that cannot be accurately captured using conventional circuit models. To address this challenge, this study introduces a novel hybrid modeling framework that combines Artificial Neural Networks (ANN) with discrete transfer functions $H(z)$ for accurately modeling the unit cell in wideband systems. Specifically, the proposed framework allows a direct prediction of the $H(z)$ coefficients from the S_{12} data obtained from a full-wave Computer Simulation Technology (CST) simulation. The proposed framework aims to bridge the electromagnetic theory and circuit theory, which are considered to be complex, by representing the unit cell behavior using computationally efficient $H(z)$ modeling. The results show that the proposed framework can accurately capture the sharp resonant characteristics of the RIS unit cell. The proposed hybrid framework achieves a performance improvement of 6 dB in Root Mean Square Error (RMSE) in comparison with the basic fitting model over all the Ka-band frequencies (30–40 GHz).

1. INTRODUCTION

The significant increase in data traffic has pushed the move towards higher frequency bands, such as millimeter wave (mm-wave) and terahertz (THz) frequencies, to compensate for the spectrum scarcity [1]. However, network deployment with such high frequencies brings several challenges required to be overcome. In particular, higher frequencies face significant propagation loss [2]. To address this propagation loss of high frequencies, researchers have proposed the use of Reconfigurable Intelligent Surfaces (RISs) [3–6]. However, RIS needs unit cell characterization to complete the design [6]. Therefore, developing the accurate modeling of the RIS unit cell becomes crucial [7]. This challenge is because RIS unit cells in wideband applications experience highly dispersive and strongly coupled electromagnetic behavior, which indeed cannot be captured by conventional circuit models [8].

However, when dealing with complex unit cell structures and their frequency-dependent behaviors, the traditional circuit models, including the simulation program with integrated circuit emphasis (SPICE) [9] and advanced design system (ADS) [10], encounter several limitations [10].

One major issue related to these conventional models is that they yield an infinite number of possible solutions and hence become challenging to identify the correct representation. Furthermore, they face a considerable challenge to accurately fit multi-resonant responses across bandwidths and hence leading to poor prediction performance, particularly at wideband frequencies. Another limitation is that they rely on static lumped-element assumptions based on RLC networks, which are valid only for a narrow bandwidth. More presciently, the RLC-based approach cannot fully account for dispersion effects and the time-varying behaviors that occur in real-word scenarios. Therefore, given the above limitations, there is a need to develop an efficient modeling approach that has the capability to accurately capture the complex multi-resonance characteristics of RIS unit cells.

To achieve this goal, this study proposes a new hybrid approach that combines the artificial neural networks (ANNs) with Digital Signal Processing (DSP)-based discrete z-transfer function $H(z)$ modeling. In particular, the proposed approach uses an ANN to predict $H(z)$ coefficients directly using the S_{12} parameter obtained from the Computer Simulation Technology (CST) simulation. It enables robust parameter extraction even for structures exhibiting many transmission nulls across Ka-band [11]. In contrast to traditional models, the proposed hybrid model can handle highly nonlinear, multi-dimensional data [10]. The proposed framework establishes a rigorous bridge between the complex electromagnetic theory and circuit theory. It is achieved by taking the advantages of the RIS unit cell behavior to effectively represent $H(z)$ in the frequency do-

* Corresponding author: Taha Ahmed Elwi (taelwi82@nahrainuniv.edu.iq).

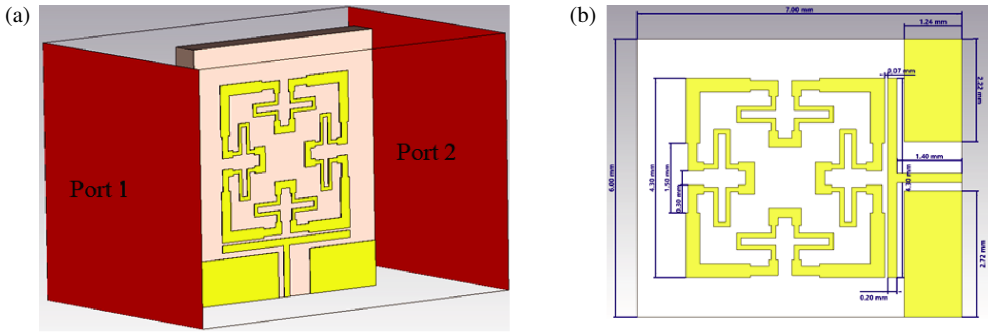

FIGURE 1. Illustration of the proposed RIS unit cell design where (a) denotes the simulation environment and (b) represents the unit cell dimensions.

main. Furthermore, the proposed ANN with a DSP-based z-transform approach treats the unit cell structure as a discrete-time dynamic system, which enables direct analysis in the z-domain, where poles, zeros, stability, and frequency responses can be evaluated across a wide band rather than at a single static operating point. This approach allows a deeper insight into signal propagation, phase, and group delay while also enabling optimization and digital filtering-based compensation strategies that traditional circuit models cannot provide.

The results show that the proposed approach can accurately capture the multi-resonant characteristics of the RIS unit cell. In addition, the results demonstrate that the proposed approach provides excellent agreement between hybrid predictions and CST full-wave simulations with less than 1.2 dB in Root Mean Square Error (RMSE). Furthermore, the results demonstrate that the proposed hybrid approach achieves a performance improvement of 6 dB in RMSE in comparison with the basic fitting $H(z)$ model across the considered Ka-band frequency range. Overall, the proposed approach provides a systematic bridge between full-wave electromagnetic analysis and practical circuit-level implementations, thereby significantly clarifying the essential requirements for an effective RIS design.

The remainder of this study is organized as follows. Section 2 describes the methodology used in this study, with the unit cell design. In addition, the proposed hybrid z-transform-based ANN approach is also provided. Section 3 discusses the results of the direct $H(z)$ and the proposed hybrid models. Finally, Section 4 concludes the study.

2. METHODOLOGY AND MODELING

This section provides the methodology developed in this study as follows.

2.1. Unit Cell Design and Full-Wave Simulation

In this study, a unit cell with a multi-order Minkowski fractal geometry [12, 13] is designed to operate in the Ka-band. The structure of the proposed unit cell is shown in Fig. 1, where Fig. 1(a) denotes the simulation environment, and Fig. 1(b) represents the dimensions of the unit cell. The proposed design uses a series of space-filling modifications applied along the current path to increase the electrical length of the unit cell while maintaining physical size compactness. In particular, the unit cell is composed of four symmetrically arranged fractal arms that are connected to provide a continuous current flow across the structure. In addition, each arm of the unit cell consists of three connected segments with a distinctive indentation introduced at each stage. These fractal indentations drive the surface currents to take a longer meandering path while also acting as capacitive discontinuities. As a result, the effective inductance of the resonator increases without increasing the size of the structure. The compact coupling structure guarantees that energy is distributed equally to all fractals at the center of the unit cell. Furthermore, the lower part of the unit cell contains the feeding region and consists of two rectangular stubs separated by a narrow gap. A T-shape is placed below the four fractal arms and between the two rectangular stubs to increase the electric field concentration, thereby increasing the effective capacitance and enhancing the efficiency of energy transfer. Overall, despite the electrically compact dimensions of the structure, resonance in the Ka-band is achieved through the combination of symmetric current loops, strong capacitive gaps, and Minkowski fractal loading. The proposed unit cell is suitable for RIS filters and small resonant sensors because it exhibits sharp notch features and can provide high-quality resonances.

A full-wave CST simulation was used to simulate the proposed unit cell. The electric and magnetic fields were distributed appropriately along the x and z axes, respectively. The two waveguide ports placed along the y-axis allow electromagnetic waves to propagate. The proposed unit cell was composed of a metallic layer with a Roger AD 430 substrate of $7 \times 6 \times 0.508\,\text{mm}^3$ dimensions. The substrate features a dielectric constant of 4.3 and a low loss tangent of 0.003, making it suitable for high-frequency band applications.

Figure 2 shows the magnitude and phase responses of the S_{12} parameter of the unit cell obtained from the CST simulation. Fig. 2(a) clearly illustrates that the unit cell exhibits multiple transmission nulls. Fig. 2(b) shows the continuous phase in degrees as a function of the Ka-bands operating frequency range.

2.2. The Proposed Hybrid z-Transform Based ANN Approach

This study proposes a hybrid approach based on ANN and DSP z-transform to obtain an explicit and straightforward solution for RIS unit cell characterization. That current study focuses on establishing the theoretical framework and compu-

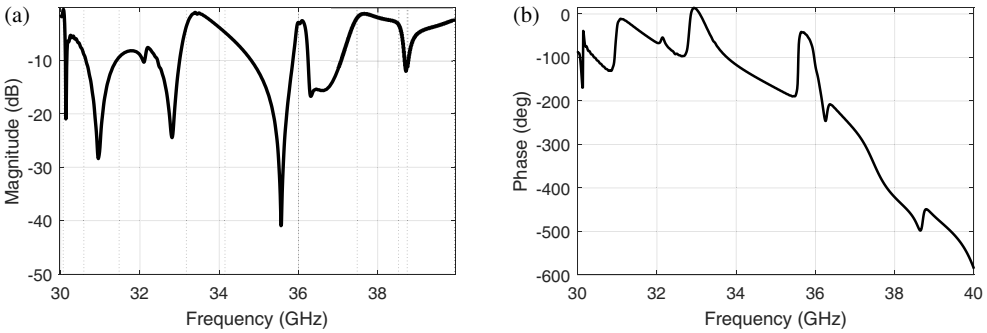

FIGURE 2. Magnitude and phase responses of S_{12} parameter obtained from the CST simulation. (a) Magnitude response of the S_{12} parameter. (b) Phase response of the S_{12} parameter.

tational validation of the hybrid modeling approach based on ANN and $H(z)$. However, circuit modeling of RIS unit cells is typically validated through electromagnetic simulations, e.g., CST, before fabrication. The main contribution of the present study is based on demonstrating that the hybrid approach of ANN for predicting the $H(z)$ coefficient is feasible. Moreover, the proposed hybrid framework is accurate in comparison with the conventional fitting methods, especially when dealing with multi-resonance designs over wide frequency ranges.

The methodology of the proposed framework comprises the following main stages: (1) data generation and collection, (2) pre-processing and ANN implementation, (3) discrete transfer function fitting, and (4) pole-zero analyses. The frequency-sampled S_{12} data obtained from the CST simulation was 1001 points over the frequency range of 30–40 GHz. For the ANN architecture, this study considers a single hidden layer with 32 feedforward network neurons. Besides, the Levenberg-Marquardt backpropagation training algorithm was considered. The frequency was normalized to be between $[0, 1]$ range. The methodology of this study is illustrated in Fig. 3.

2.2.1. Data Generation and Collection

S-parameters provide a general framework for characterizing electromagnetic behavior, enabling seamless post-processing and integration into various designs. A key advantage is that electromagnetic simulation tools, such as CST, routinely generate S-parameters that can be directly validated against experimental measurements, facilitating model verification. These capabilities have established frequency-domain S-parameter analysis as a fundamental approach for electrical link characterization and system-level performance evaluation. The frequency-domain approach has been adopted for high-speed digital analysis and signal integrity characterization. However, for comprehensive design validation, S-parameters must often be transformed into the time domain to enable direct comparison with time-domain metrics, such as eye diagrams and bit error rates (BER). These S-parameters must be transformed either using inverse fast Fourier transform (IFFT) techniques [14] or through a rational function approximation using equivalent circuit synthesis. Vector fitting algorithms and pole-residue decomposition methods were used for this purpose. Regardless of the transformation method employed, the accuracy and quality

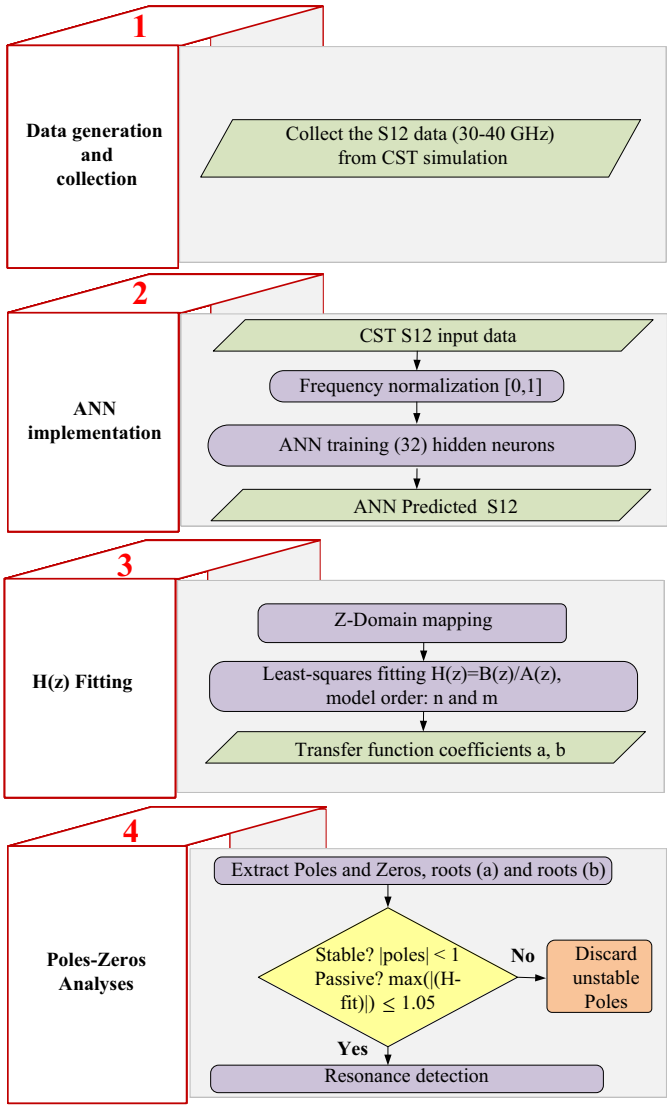

FIGURE 3. Flowchart of the proposed hybrid model based on ANN and z-transformation for RIS unit cells characterization.

of the measured or simulated S-parameters are essential and must satisfy criteria such as passivity and stability.

Full-wave electromagnetic simulations of the RIS unit cell were performed in CST Microwave Studio over the 30–40 GHz band, producing complex S_{12} transmission coefficient

TABLE 1. Examining different sets of poles and zeros orders.

n	*m*	Passivity	Stability (Max pole raduis)	RMSE (dB)	Status
4	3	✓	✓(0.9625)	6.224	Underfitting
4	4	✓	✓(0.9572)	6.242	Underfitting
8	7	✓	*x* (1.0061)	2.992	Unstable
8	8	✓	✓(0.9949)	2.026	Not optimal
10	**9**	✓	✓(0.9797)	**1.417**	**Optimal**
10	10	✓	✓(0.9797)	1.548	Overfitting

data. This discrete sampling inherently produces a discrete-frequency representation of the electromagnetic response, which can be accurately described by a rational transfer function $H(z)$ that relates the input and output responses in the Z-domain. However, the raw CST output often contains numerical noise and small fluctuations arising from mesh discretization and broadband solver limitations. To address this issue, an ANN is applied. Further discussion regarding ANN implementation is provided in the following subsection.

2.2.2. Preprocessing and ANN Implementation

In this study, the complex S_{12} transmission coefficient is used as the input data for the ANN model, which was collected from electromagnetic CST simulations as mentioned above. In particular, an ANN is used to suppress noise through learned nonlinear smoothing and rapid prediction of clean S_{12} responses. By learning the underlying physical trend of the transmission behavior, the ANN can generate a smooth, noise-free approximation of S_{12}, which is crucial for an accurate z-domain mapping and least-squares $H(z)$ fitting. This preprocessing step prevents the emergence of unstable or nonphysical poles, improves passivity compliance, and ensures that the extracted resonances are physically meaningful. Consequently, the ANN significantly enhanced the reliability of the pole-zero analyses and accelerated the overall RIS characterization process.

Frequency normalization was applied before feeding the data into the ANN to improve the training stability and accuracy. Typically, neural networks learn patterns more effectively when the input values are scaled to a consistent range [0–1]. By normalizing the frequency, the ANN trains faster, avoids numerical issues, and produces smoother and more reliable S_{12} predictions. To this end, a feedforward neural network with 32 hidden neurons was used to predict S_{12} real and imaginary components from the normalized frequency. It created a smooth and continuous model of the S_{12} response.

2.2.3. Transfer Function H(z) Fitting

The discrete transfer function $H(z)$ is a useful mathematical tool for digital signal processing and control systems because it can be efficiently used for analyzing and modeling discrete-time linear systems [15]. This stage of the methodology was used to convert the ANN prediction to a discrete transfer function $H(z)$. $H(z)$ can model the frequency-dependent behavior of a system with poles and zeros. Noting that the digital frequency is mapped to $[0, \pi]$ for Z-domain representation.

This study considers a system identification approach based on the z-transform. The frequency-sampled S_{12} data from the CST simulation was fitted to a discrete-time rational transfer function so that the general $H(z)$ is given in [16]

$$H(z) = \frac{B(x)}{A(z)} = \frac{\sum_{k=0}^{m} b_k z^{-k}}{1 + \sum_{k=1}^{n} a_k z^{-k}}, \tag{1}$$

where b and a are the numerator and denominator coefficients of the transfer function $H(z)$, respectively; parameter m denotes the number of zeros (numerator order); and n denotes the number of poles (denominator order). Furthermore, the fitted $H(z)$ is evaluated across all frequency ranges to visualize how well the fitted model matched the original CST simulation data.

2.2.4. Poles and Zeros Analyses

This is the final stage, where the poles (roots of the denominator) and zeros (roots of the numerator) of $H(z)$ are extracted. The frequency-dependent behavior of a system with poles and zeros was modeled using $H(z)$, which directly corresponds to the S_{12} data. The fitted $H(z)$ is validated for stability and passivity, where the system is considered to be stable if all poles satisfy $|poles| < 1$. The passivity was evaluated and verified by ensuring that $|H|$-fit ≤ 1.05 over the frequency bands considered. The fitting accuracy was quantified using the RMSE in the dB domain. For resonant structures, the number of poles (n = poles) typically corresponds to the number of expected resonances in the frequency band and the number of zeros (m = zeros). This study starts with lower orders and incrementally increases poles and zeros while monitoring RMSE and condition number. The proposed approach is validated using multiple criteria approaches, such as stability, passivity, and RMSE, as discussed above. The RMSE formulation is given as [17]

$$\text{RMSE} = \sqrt{\frac{1}{n}\sum_{i=1}^{n}\left(y_i - \hat{y}_i\right)^2}. \tag{2}$$

Noting that the number of poles n and zeros m selection for the $H(z)$ was determined based on the unit cell structure, which is based on several resonances. Therefore, the ranges of n and m were selected within the interval $[4, 10]$. The values inside the range were tested across different sets of n and m orders, as

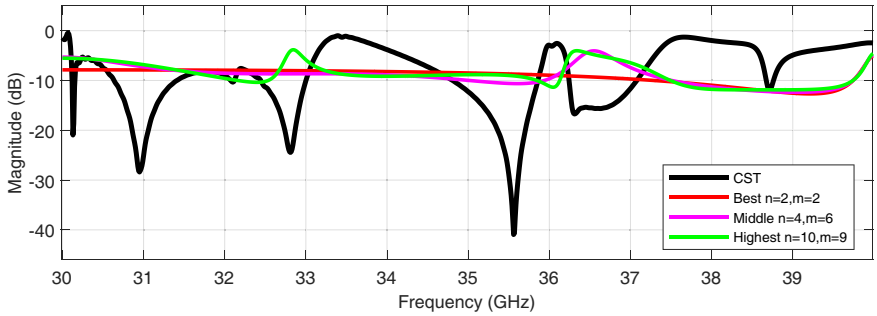

FIGURE 4. Comparison of S_{12} magnitude as a function of frequency for data obtained from CST with $H(z)$ considering different values of n and m.

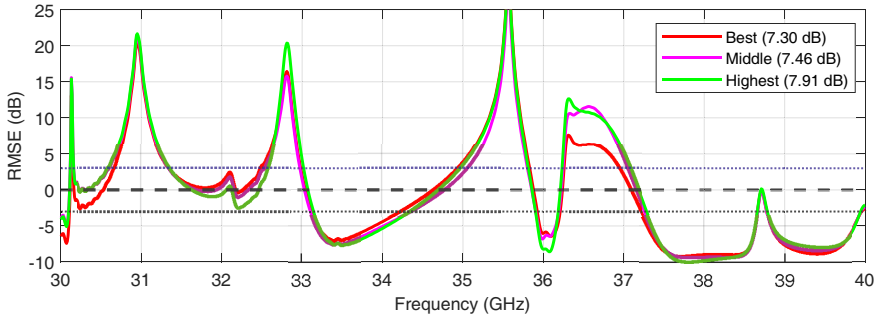

FIGURE 5. RMSE as a function of frequency from CST with $H(z)$.

demonstrated in Table 1. Besides, a least-squares fitting problem was used to obtain the values and locations of these orders, which are denoted by numerator coefficients (b) and denominator coefficients (a) that best match the original CST data. On the other hand, the pole corresponded to a natural resonant frequency. It relates to maximizing interchange between the electric and magnetic energy.

As shown in the table, the selection of n and m is based on finding the best trade-off among model accuracy, stability, and complexity. Lower-order models exhibit underfitting behavior, as the limited number of poles and zeros is insufficient to capture the underlying system dynamics, resulting in higher RMSE values despite stable pole locations. It is also important to note that models with higher orders would overfit the data and increase the RMSE. This is because it will fit noise instead of the signal. Therefore, the selection of an optimal configuration would be based on finding stable dynamics with the poles that are located within the unit circle and also have the lowest RMSE. It implies obtaining an accurate system representation and ensuring reliable communication performance by avoiding both underfitting and overfitting effects.

The locations of the poles determine the system stability: poles located inside the unit circle in the z-domain indicate a stable system in which dissipative mechanisms dominate. The poles are precisely placed on the unit circle. This implies marginal stability, in which the energy stored and energy dissipated are balanced. On the other hand, if the poles are placed outside the unit circle, it implies that there is instability, which indicates that the stored reactive energy exceeds the system losses, hence would lead to unbounded growth in the oscillations. Therefore, the placement of the poles provides a framework for illustrating the stability characteristics, energy exchange, and resonance behavior, hence making them valuable for analyzing unit cell structures.

3. RESULTS AND DISCUSSION

This section presents the performance evaluation using the direct $H(z)$ method and the proposed hybrid approach.

3.1. Results of Direct *H*(*z*) Method

Figures 4 and 5 show a comparison of S_{12} magnitude and RMSE as a function of frequency for data obtained from CST with $H(z)$ considering different values of n and m, respectively. The results showed that increasing the order numbers n and m increased the RMSE and failed to achieve the desired fitting model. The results demonstrate that direct $H(z)$ fitting creates an RMSE of more than 7 dB. This is because direct $H(z)$ fitting methods are constrained by model order selection and fail for complex unit cell structures, yielding high RMSE values. In particular, for multi-resonant designs, the S_{12} data from the CST are too complex for simple fitting models. Specifically, the transfer function $H(z)$ obtained through direct fitting failed to estimate the S_{12} data. This is due to the complexity characteristic of the unit cell that has multiple transmission nulls at high frequencies. As such, incorrect amplitude and phase values can be provided by RIS. As a consequence, it will lead to inaccurate beamforming and steering capability and hence degrade the communication system performance. Therefore, there is still a need to find a feasible model to address the above issues.

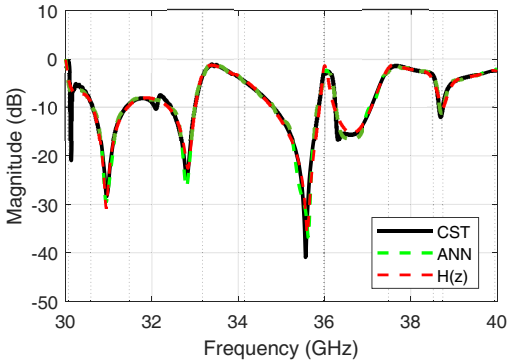

FIGURE 6. Comparison of S_{12} magnitude of data obtained from CST, ANN, and $H(z)$ $n = 10$ poles, $m = 9$ zeros.

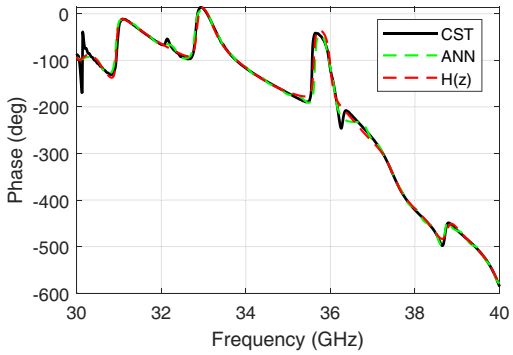

FIGURE 7. Comparison of the magnitude and phase responses of data obtained from CST, ANN, and $H(z)$.

3.2. Performance Evaluation of the Proposed Hybrid Method

An accurate characterization of the transmission coefficient and phase of electromagnetic unit cells is essential for designing broadband metasurfaces, frequency-selective surfaces (FSS), and RIS [7].

To accurately capture the multiple closely spaced resonances and notches observed in the unit-cell S_{12} spectrum, a higher-order rational fit ($n = 10$ poles, $m = 9$ zeros) was used. The proposed hybrid model provides an excellent fit. In particular, the extracted $H(z)$ achieved an RMSE of less than 1.2 dB relative to CST simulation, demonstrating frequency domain accuracy.

Figure 6 shows a comparison of the magnitude and phase responses from CST, ANN, and $H(z)$. In particular, Fig. 6 shows a comparison of S_{12} magnitude data obtained from CST, ANN prediction model, and $H(z)$ at $n = 10$ poles and $m = 9$ zeros. The results show that the magnitude response exhibits five distinct resonances centered at 31, 33, 35.8, 36.2, and 39 GHz. The deep nulls are approximately 31 and 35 GHz, and peaks near 0 dB at approximately 34 GHz, and 37–38.5 GHz. The results showed excellent agreement among all three models across the frequency range. The curves were nearly identical, with all three tracking the same pattern of peaks and deep notches. The results show that the ANN model can effectively predict the $H(z)$ transfer function coefficients of the frequency response with high accuracy compared with the full-wave CST electromagnetic simulation.

Figure 7 shows the S_{12} phase response comparison among the CST simulation, ANN model, and $H(z)$ transfer function across 30–40 GHz. The results demonstrated excellent agreement among the three methods. The phase decreased almost linearly from approximately $0°$ at 30 GHz to approximately $-600°$ at 40 GHz. The results confirm that the hybrid model accurately captures not only the magnitude but also the phase characteristics of the system, thus validating its effectiveness for unit cell modeling.

Figure 8 shows the results of the group delay as a function of frequency. The group delay of a system is defined as the negative derivative of the phase response with respect to angular frequency. The results show that there is group delay variation over the frequency range considered of about -5 ns at 31 GHz

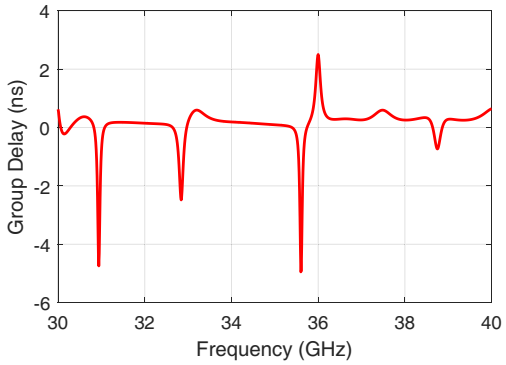

FIGURE 8. Illustration of the group delay time in nano seconds (ns) based on the fitting model $H(z)$.

and 35.7 GHz. These results correspond to the sharp transmission nulls, which are observed in the S_{12} magnitude response. In addition, a positive peak of approximately 3 ns occurred near 36 GHz, resulting in a peak-to-peak excursion exceeding 7 ns. Such extreme Group Delay Variation (GDV) causes significant signal distortion in wideband systems. Compared to typical symbol periods (approximately 1 ns at 1 Gbaud), this level of GDV introduces substantial inter-symbol interference (ISI).

Figure 9 shows results for both the passivity and pole/zero distributions. Specifically, the results in Fig. 9(a) demonstrate that the proposed hybrid model achieves passivity based on the number of poles and zeros.

Moreover, Fig. 9(b) shows the mapping of poles and zeros of the fitted $H(z)$ in the z-domain. This map can be considered a fundamental tool for frequency response characteristics, hence analyzing discrete/time system stability. The results show that the unit circle can serve as a stability boundary. To this end, the systems are considered to be stable if all poles are located inside this circle so that $|poles| < 1$. These presented results confirm the system stability. Besides, the results also demonstrate that there are several poles located near the unit circle boundary with $|poles| \approx 0.95$–0.99. It implies a high-quality factor (high-Q) resonances, which corresponds to the sharp resonant characteristics observed in the S_{12}, at approximately 31 GHz and 36 GHz. The results show a distribution of 10 poles and 8 out of 9 zeros. This is due to the results of a polynomial with m coefficients, which have a degree of $m - 1$, resulting in $m - 1$

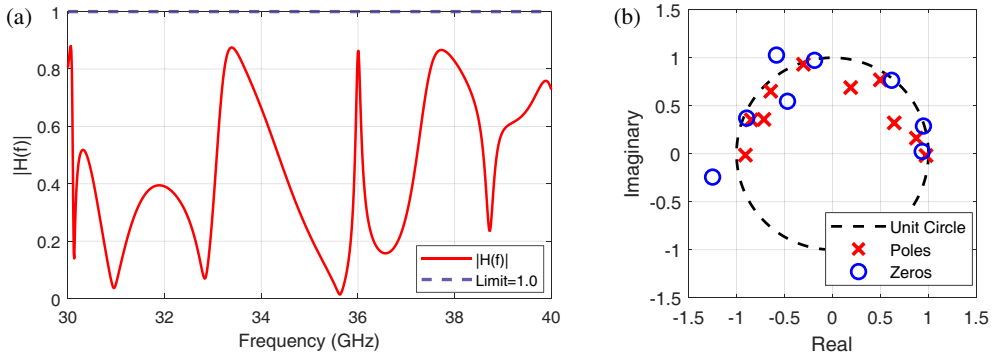

FIGURE 9. Illustration of the transfer function passivity and poles, zeros distribution. (a) System passivity as a function of frequency in GHz. (b) Distribution of the poles and zeros of the transfer function in the z-plane.

TABLE 2. Comparison of the proposed approach with the related works.

Ref.	Method	Modeling approach	Frequency range	Input data	RMSE (dB)	Time consuming
[18]	ADS	Equivalent circuit model and ADS	3.5 GHz	S-parameters	NP	Slow
[19]	Equivalent RLC circuit	Analytical formulas	26–40 GHz	Geometry with EM simulation	NP	Medium
[17]	Machine learning	CNN-ResNet surrogate model	6.0–16.0 GHz	Binary element	3	Fast
[20]	ADS	RLC circuit optimization	Wideband (10–40 GHz)	S-parameters	NP	Slow
This study	Proposed (ANN-$H(z)$)	Hybrid (ANN and DSP)	30–40 GHz	S-parameters	1.417	Fast

roots zeros that were positioned inside and on a unit circle. The distribution of poles and zeros reflects the bandpass filtering characteristics of the RIS unit cell over all the Ka-band considered.

Ten poles were selected for the circuit modeling based on the behavior of the imaginary part of mutual impedance Z_{12}. Specifically, the points along the frequency axis are observed, where the imaginary component of Z_{12} crosses zero, each of which indicates the presence of a resonant mechanism in the unit cell. Because pole locations in the rational model correspond directly to the physical resonances of the electromagnetic structure, identifying all such zero-crossing regions ensures that the model captures every significant resonant response. The number of poles quantifies the sharpness of the resonances. Table 2 provides a comparison of the proposed approach with related works.

4. CONCLUSION

This study proposed a hybrid approach combining ANN with z-transformation to address the limitations associated with conventional circuit modeling for analyzing the RIS unit cell. The proposed hybrid approach achieved the direct prediction of $H(z)$ coefficients using an ANN model. The S_{12} data, which were used as the input for the ANN, were obtained from a full-wave CST simulation. The results showed that the proposed hybrid approach accurately captured the sharp resonant characteristics of the RIS unit cell and achieved a performance improvement of 6 dB in RMSE compared with the basic fitting $H(z)$ model across the Ka-band frequency range (30–40 GHz). The proposed hybrid ANN and DSP-based z-transform technique enabled direct analysis in the z-domain, where poles, zeros, stability, and frequency responses can be accurately evaluated across a wide band rather than at a single static operating point. The proposed approach provides a deeper insight into signal propagation, phase delay, group delay, dispersion effects, and radiation performance, which traditional circuit models cannot provide. Consequently, the proposed approach delivers a higher resolution, stronger physical interpretation of wave behavior, and a more reliable framework for modeling real-world RIS structures. While the current study aimed to establish a computational framework through simulation validation, future work could focus on considering experimental validation using fabricated RIS unit cell prototypes.

REFERENCES

[1] Xiao, M., S. Mumtaz, Y. Huang, L. Dai, Y. Li, M. Matthaiou, G. K. Karagiannidis, E. Björnson, K. Yang, C.-L. I, and A. Ghosh, "Millimeter wave communications for future mobile networks," *IEEE Journal on Selected Areas in Communications*, Vol. 35, No. 9, 1909–1935, 2017.

[2] Kumar, A., S. Sharma, M. H. Kumar, and G. Singh, "RIS-assisted terahertz communications for 6G networks: A comprehensive overview," *IEEE Access*, Vol. 13, 96 337–96 364, 2025.

[3] Alsabah, M., M. A. Naser, B. M. Mahmmod, S. H. Abdulhussain, M. R. Eissa, A. Al-Baidhani, N. K. Noordin, S. M. Sait, K. A. Al-Utaibi, and F. Hashim, "6G wireless communications networks: A comprehensive survey," *IEEE Access*, Vol. 9, 148 191–148 243, 2021.

[4] Liaskos, C., S. Nie, A. Tsioliaridou, A. Pitsillides, S. Ioannidis, and I. Akyildiz, "A new wireless communication paradigm through software-controlled metasurfaces," *IEEE Communications Magazine*, Vol. 56, No. 9, 162–169, 2018.

[5] Kisseleff, S., W. A. Martins, H. Al-Hraishawi, S. Chatzinotas, and B. Ottersten, "Reconfigurable intelligent surfaces for smart cities: Research challenges and opportunities," *IEEE Open Journal of the Communications Society*, Vol. 1, 1781–1797, 2020.

[6] Wu, Q., S. Zhang, B. Zheng, C. You, and R. Zhang, "Intelligent reflecting surface-aided wireless communications: A tutorial," *IEEE Transactions on Communications*, Vol. 69, No. 5, 3313–3351, 2021.

[7] Rafique, A., N. U. Hassan, M. Zubair, I. H. Naqvi, M. Q. Mehmood, M. D. Renzo, M. Debbah, and C. Yuen, "Reconfigurable intelligent surfaces: Interplay of unit cell and surface-level design and performance under quantifiable benchmarks," *IEEE Open Journal of the Communications Society*, Vol. 4, 1583–1599, 2023.

[8] Yesilyurt, O. and G. Turhan-Sayan, "Metasurface lens for ultra-wideband planar antenna," *IEEE Transactions on Antennas and Propagation*, Vol. 68, No. 2, 719–726, 2020.

[9] Kuznetsov, V., "Microstrip line modeling taking into account dispersion using a general-purpose SPICE simulator," *Journal of Low Power Electronics and Applications*, Vol. 15, No. 3, 42, 2025.

[10] Mayaram, K., D. C. Lee, S. Moinian, D. A. Rich, and J. Roychowdhury, "Computer-aided circuit analysis tools for RFIC simulation: Algorithms, features, and limitations," *IEEE Transactions on Circuits and Systems II: Analog and Digital Signal Processing*, Vol. 47, No. 4, 274–286, 2000.

[11] Wang, Z., S. Hu, L. Gu, and L. Lin, "Review of Ka-band power amplifier," *Electronics*, Vol. 11, No. 6, 942, 2022.

[12] Dileep, A., P. V. Abhilash, V. Joy, H. Singh, and R. U. Nair, "Metamaterial absorber based on minkowski fractal patch for stealth applications," in *2020 IEEE International Conference on Electronics, Computing and Communication Technologies (CONECCT)*, 1–4, Bangalore, India, 2020.

[13] Anwer, A. I., M. Alibakhshikenari, T. A. Elwi, B. S. Virdee, L. Kouhalvandi, Z. A. A. Hassain, M. Soruri, N. T. Tokan, N. O. Parchin, C. H. See, and P. Livreri, "Minkowski based microwave resonator for material detection over sub-6 GHz 5G spectrum," in *2023 2nd International Conference on 6G Networking (6GNet)*, 1–4, Paris, France, 2023.

[14] Pfister, H. D., *Discrete-time Signal Processing*, http://pfister.ee.duke.edu/courses/ece485/dtsp.pdf, 2017.

[15] Zhang, Y., N. Feng, J. Zhu, G. Xie, L. Yang, and Z. Huang, "Z-transform-based FDTD implementations of biaxial anisotropy for radar target scattering problems," *Remote Sensing*, Vol. 14, No. 10, 2397, 2022.

[16] Oppenheim, A. V., *Discrete-time Signal Processing*, 1999.

[17] Liu, X., P. Nian, Y. Zhang, Y. Ren, Y.-X. Guo, Y.-C. Gao, and B. Chen, "Machine learning-based RCS prediction for metasurface-integrated cavity structures," *Progress In Electromagnetics Research M*, Vol. 136, 68–76, 2025.

[18] Araghi, A., M. Khalily, M. Safaei, A. Bagheri, V. Singh, F. Wang, and R. Tafazolli, "Reconfigurable intelligent surface (RIS) in the sub-6 GHz band: Design, implementation, and real-world demonstration," *IEEE Access*, Vol. 10, 2646–2655, 2022.

[19] Liu, Y., F. Wang, T. Zhao, X. Weng, X. Xi, and K.-D. Xu, "Spoof surface plasmon polariton-based E-plane waveguide bandpass filters using equivalent circuit method," *IEEE Transactions on Microwave Theory and Techniques*, Vol. 74, No. 1, 858–868, 2026.

[20] Hossain, M. A., M. L. Hakim, M. A. Alawad, and M. T. Islam, "DNG metamaterial-embedded multilayer FSS for substrate-specific EM profiling and ultra-wideband mm-wave suppression," *Ain Shams Engineering Journal*, Vol. 17, No. 1, 103865, 2026.